

Magnetization studies in the rare-earth orthochromites. V. TbCrO_3 and PrCrO_3 †

J. D. Gordon, R. M. Hornreich, and S. Shtrikman

Department of Electronics, The Weizmann Institute of Science, Rehovot, Israel

B. M. Wanklyn

Clarendon Laboratory, Oxford, England

(Received 13 March 1975)

The spontaneous magnetization and principal susceptibilities of the rare-earth orthochromites TbCrO_3 and PrCrO_3 are studied in the temperature range $4.2^\circ\text{K} \leq T \leq T_N$. For the case of PrCrO_3 the field dependence of the magnetization at $T = 4.2^\circ\text{K}$ is also measured. For both materials, it is found that (a) the Cr^{3+} spin system orders in a $\Gamma_2 (F_x)$ mode, (b) no spin reorientation or compensation point occurs in the observed temperature range, and (c) the effective g tensor of the rare-earth electrons is essentially zero along the c crystallographic axis. The experimental data are interpreted using a doublet model for the rare-earth ion. For TbCrO_3 , $T_N = 167^\circ\text{K}$, $g_a = g_b = 12.6$, the effective field exerted by the ordered Cr^{3+} spin system on a Tb^{3+} moment at 0°K is equivalent to a splitting of $\Delta_0 = 1.8^\circ\text{K}$ and the crystal-field splitting $D = 14^\circ\text{K}$. The canting angle α of the Cr sublattice is unusually small (less than 5 mrad). For PrCrO_3 , $T_N = 237^\circ\text{K}$, $g_a = 2.9$, $g_b = 3.3$, $\Delta_0 = 17^\circ\text{K}$, $D = 55^\circ\text{K}$, and $\alpha = -18$ mrad. The negative sign reflects the antiparallel alignment of the Cr and Pr contributions to the spontaneous magnetization.

INTRODUCTION

The rare-earth orthochromites TbCrO_3 and PrCrO_3 crystallize in an orthorhombically distorted perovskite structure (space group $Pbnm$) with four formula units per unit cell.¹ The exchange coupling between the Cr^{3+} nearest neighbors in these compounds is predominantly antiferromagnetic and the Cr^{3+} spins order spontaneously at Néel temperatures of $T_N = 167^\circ\text{K}$ (TbCrO_3) and 237°K (PrCrO_3). Below their respective Néel points, both materials exhibit weak ferromagnetic moments. Extensive neutron-diffraction studies^{2,3} on TbCrO_3 have shown that the Cr^{3+} spin structure is, in the notation of Koehler *et al.*⁴ and Bertaut,⁵ primarily G_z below T_N and belongs to the Γ_4 representation of $Pbnm$. This implies that the weak ferromagnet component of the Cr^{3+} moments lies along the a crystallographic axis.⁵ For PrCrO_3 , on the other hand, neutron-diffraction studies indicate that the Cr^{3+} spin structure is predominantly G_x (belonging to the Γ_2 representation) at 4.2°K . This then implies that the weak ferromagnetic moment of PrCrO_3 lies along the c crystallographic axis at liquid-helium temperature.

Turning to the rare-earth ions, the Tb^{3+} spins in TbCrO_3 order antiferromagnetically at 3.05°K .³ Below this temperature the Tb^{3+} spin system exhibits an $a_x g_y$ structure associated with the wave vector $\vec{k} = (0, \frac{1}{2}, 0)$ and, for a Hamiltonian consisting of bilinear terms, is decoupled from the Cr^{3+} spin system.⁶ For $3.05^\circ\text{K} < T < T_N$, however, the Tb^{3+} spin system has an $f_x c_y$ structure belonging to Γ_4 and is coupled to the ordered Cr^{3+} spin system.³

Specific-heat measurements⁷ have shown that the Pr^{3+} spins in PrCrO_3 do not order spontaneously down to 1.5°K . Thus we expect that the Pr^{3+} moments will exhibit an induced spin structure belonging to the same representation as the ordered Cr^{3+} spin system below T_N .

The electronic ground states of the even electron ions Tb^{3+} and Pr^{3+} are 7F_6 and 3H_4 , respectively. The crystalline field can then split each of these states into $2J+1$ singlets. This complete lifting of the degeneracy is possible due to the relatively low symmetry of the rare-earth sites.¹ For the case of HoCrO_3 , it has been shown⁸ that the splitting between the two lowest-lying singlet states is small and that they are relatively isolated from the other states. We shall show that the same type of model, in which only two crystal-field states are considered, will also account for the observed magnetic properties of TbCrO_3 and PrCrO_3 .

EXPERIMENTAL

The spontaneous magnetization and principal magnetic susceptibilities of selected flux-grown single crystals of TbCrO_3 and PrCrO_3 were measured from 4.2°K to above their respective Néel temperatures. Laue back-reflection x-ray measurements were used to select samples free of twinning or other structural imperfections. The crystals chosen for measurement purposes were small platelets in the form of parallelepipeds. Labeling the platelet edge dimensions by $l_1 > l_2 > l_3$, the TbCrO_3 sample studied had $l_1/l_2 = 3.3$, $l_2/l_3 = 3.0$. The platelet $l_2 l_3$ surface was parallel to

(110) and the [001] direction was along l_2 . For the PrCrO_3 sample, $l_1/l_3 = 3.0$, $l_2/l_3 = 2.3$, the platelet l_2l_3 surface was parallel to (001) and the [100] and [010] directions were parallel to l_2 and l_1 , respectively.

Two motor driven vibrating sample magnetometers⁹ were used for our measurements. In the first unit the sample was cooled by a stream of helium vapor and magnetic fields up to 10 kOe were available. The second employed a superconducting solenoid providing magnetic fields up to 48 kOe and the sample was immersed directly in the liquid-He bath. The reported results were compiled from (i) magnetization measurements versus temperature recorded at various fixed magnetic fields and (ii) curves of magnetization versus applied field recorded at fixed temperatures. Above 4.2 °K the temperature was controlled by means of a temperature controller operated by a magnetic valve.¹⁰ The spontaneous magnetization of TbCrO_3 below its ordering temperature $T_N = 167$ °K, and down to 4.2 °K, was found to be in the a crystallographic direction. This is in agreement with the results of powder neutron-diffraction studies.^{2,3} The spontaneous moment, corrected for demagnetization effects, is shown in Fig. 1. It was found to increase monotonically with decreasing temperature within the entire temperature range studied. The principal magnetic susceptibilities were found in the usual manner from the asymptote to the slope of the magnetization versus applied field curves for fields above approximately 500 Oe. This is necessary in order to avoid spurious contributions due to magnetic

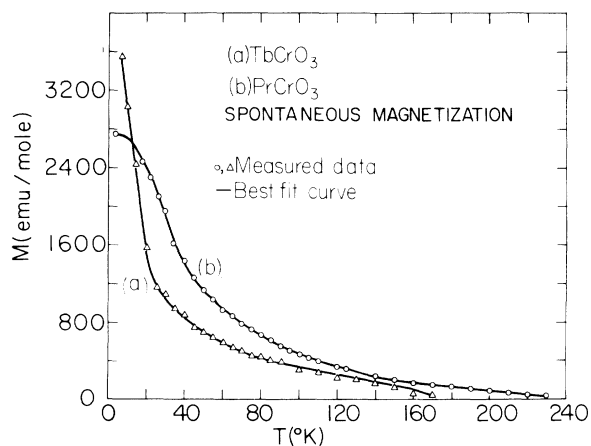


FIG. 1. Temperature dependence of the spontaneous magnetization of TbCrO_3 and PrCrO_3 . The magnetization lies along the a crystallographic axis in both cases. (The theoretical best-fit curves in Figs. 1–6 were obtained by fitting the total data for each material simultaneously, using the parameter values given in Table I).

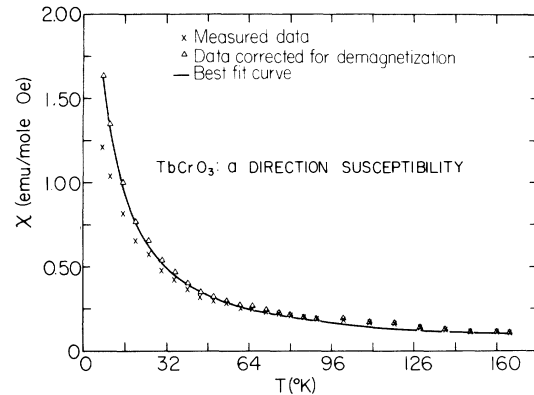


FIG. 2. Temperature dependence of the a -axis susceptibility in TbCrO_3 .

domains in materials with a spontaneous moment. The results of measurements on TbCrO_3 along the a and b crystallographic axes are shown in Figs. 2 and 3. Owing to the high susceptibility values, a demagnetizing field correction was necessary. This was done by approximating the sample by an ellipsoid with appropriate axial ratios and orientation. The corrected data are also given in Figs. 2 and 3.

The spontaneous magnetization of PrCrO_3 is given in Fig. 1. It was also found to lie along the a axis between $T_N = 237$ and 4.2 °K. This indicates that the Cr^{3+} spin structure is G_4F_x in the entire temperature range, and is not in agreement with the powder neutron-diffraction report² of a G_x mode at 4.2 °K. We shall return to this point in the final section. The a and b axis principal susceptibilities of PrCrO_3 are given in Figs. 4 and 5. For this compound and sample shape the demagnetizing corrections were small (less than 1%) and are

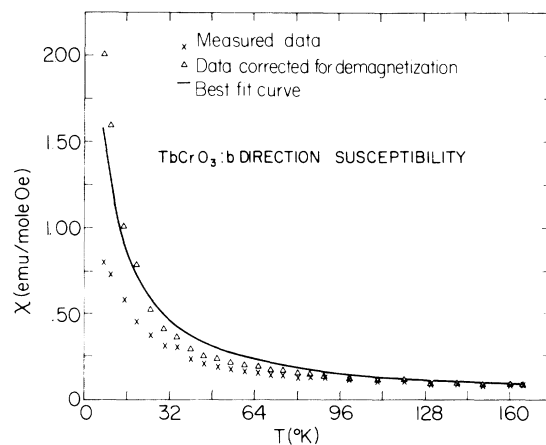


FIG. 3. Temperature dependence of the b -axis susceptibility in TbCrO_3 .

therefore not shown. Finally, in Fig. 6, the field-dependent magnetization curves along the a axes at 4.2 °K are given. The small discrepancy between the data in Fig. 6 and the $T=4.2$ °K principal susceptibilities quoted in Figs. 4 and 5 is probably due to the fact that different instruments were used for these measurements.

For both TbCrO_3 and PrCrO_3 the c axis susceptibilities are considerably smaller than those along the other two principal axes and are essentially temperature independent below 100 °K. The measured values were 7×10^{-3} and 9×10^{-3} emu/mole-Oe for TbCrO_3 and PrCrO_3 , respectively.

ANALYSIS

The following similarities exist between the magnetic properties of TbCrO_3 and PrCrO_3 : (i) The rare-earth ions of both compounds possess an even number of electrons. (ii) Their spontaneous magnetizations are both parallel to the crystallographic a axis. (iii) Their low-temperature magnetic susceptibilities exhibit the same type of anisotropy with $\chi_c \ll \chi_a, \chi_b$.

These similarities indicate that a common model can be used to analyse the properties of both TbCrO_3 and PrCrO_3 . The model chosen is essentially the same as that described elsewhere for the case of HoCrO_3 ,⁸ and we therefore restrict ourselves to a brief summary of its basic features.

For $C_3(m)$ site symmetry, the rare-earth ground state $2S+1L_J$ can be split into $2J+1$ singlets by the crystalline field. The magnetic properties of TbCrO_3 and PrCrO_3 can be understood if it is assumed that the doublet composed of the two lowest-lying singlets is relatively isolated from higher-lying levels. We use a single-ion molecular-field model in which the magnetic interactions between the Cr^{3+} and rare-earth spins and

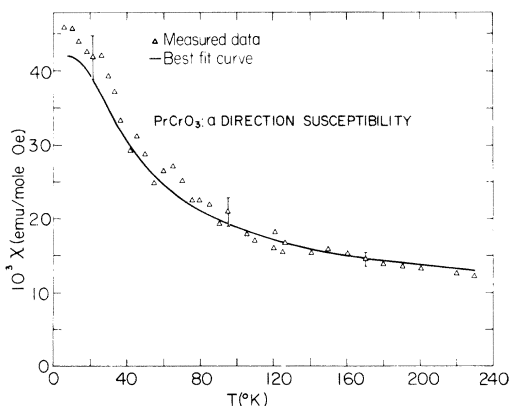


FIG. 4. Temperature dependence of the a -axis susceptibility in PrCrO_3 .

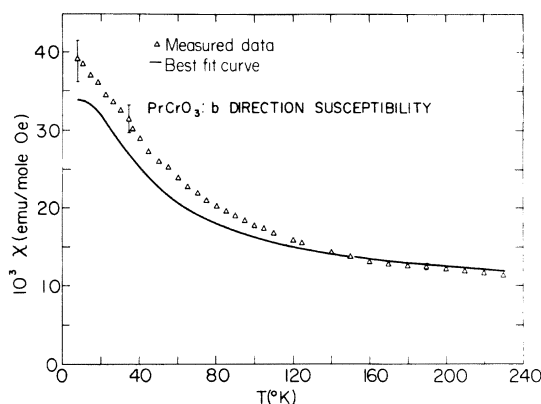


FIG. 5. Temperature dependence of the b -axis susceptibility in PrCrO_3 .

between the rare-earth spins themselves are represented by effective magnetic fields acting on the rare-earth moments. As we have seen, for TbCrO_3 and PrCrO_3 the Cr^{3+} spin structure is $F_x G_z$ and, as shown by Bertaut,⁹ this mode couples to and therefore induces an $f_x c_y$ structure for the rare-earth spin system. Thus the effective field due to the ordered Cr^{3+} spin system at a given rare-earth site lies in the $a-b$ plane. We ignore, for the moment, the rare-earth-rare-earth coupling.

For an even electron system, Griffith¹¹ has shown that the isolated doublet's effective g factor is nonzero along one axis only and is strictly zero in all perpendicular directions. For the rare-earth orthochromites, the local site symmetry restricts this axis to be either perpendicular to or within the $a-b$ crystallographic plane¹² and, from the experimental data, the latter is the appropriate choice for both TbCrO_3 and PrCrO_3 . Only in

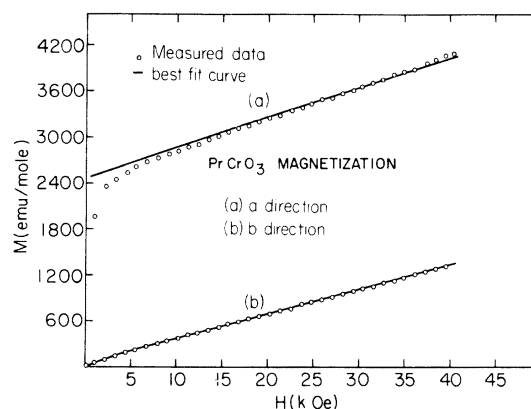


FIG. 6. Magnetic field dependence of the magnetization in PrCrO_3 at 4.2 °K along the a and b crystallographic axes.

this way can the significant Cr^{3+} -rare-earth coupling in these two compounds be understood using this model.

To determine the doublet contribution to the magnetization and susceptibility, we take the splitting $E(\bar{H})$ between the two singlet states in the form^{8,12}

$$E_{\pm}(\bar{H}) = [D^2 + (\Delta + g_a \mu_B H_a \pm g_b \mu_B H_b)^2]^{1/2}. \quad (1)$$

Here D is the crystal-field splitting, Δ is the exchange splitting caused by the effective field of the Cr^{3+} spin system, μ_B is the Bohr magneton, and g_a, g_b, H_a, H_b are the components of g and the applied field \bar{H} along the a and b axes. The \pm signs refer to the two inequivalent rare-earth sites which exhibit different splittings when an external field is applied along the b axis. Using (1), it is straightforward to show that the doublet contributions per mole to the over-all magnetization and susceptibility are given by

$$M_{0a}^{\text{RE}} = \frac{1}{2} g_a \mu_B N (\Delta/E_0) \tanh(E_0/2kT) \quad (H=0), \quad (2a)$$

$$M_a^{\text{RE}}(H_a) = \frac{1}{2} g_a \mu_B N [(\Delta + g_a \mu_B H_a)/E(H_a)] \times \tanh[E(H_a)/2kT], \quad (2b)$$

$$M_b^{\text{RE}}(H_b) = \frac{1}{2} g_b \mu_B N \{[(\Delta + g_b \mu_B H_b)/E_+(H_b)] \times \tanh[E_+(H_b)/2kT] - [(\Delta - g_b \mu_B H_b)/E_-(H_b)] \times \tanh[E_-(H_b)/2kT]\}, \quad (2c)$$

$$\chi_i^{\text{RE}} = \frac{1}{2} N g_i^2 \mu_B^2 [(D^2/E_0^2) \tanh(E_0/2kT) + (\Delta^2/2kTE_0^2) \text{sech}^2(E_0/2kT)] \quad (i = a, b). \quad (2d)$$

In (2), $E_0 = (D^2 + \Delta^2)^{1/2}$, N is Avogadro's number, and k is Boltzmann's constant.

The measured magnetization and susceptibility of TbCrO_3 and PrCrO_3 also include, of course, contributions from the Cr^{3+} spins. Assuming that the canting angle, i.e., the angle α between the Cr^{3+} sublattice moment and the c axis, is temperature independent,^{13,14} the total a direction spontaneous magnetization moment is

$$M_a = M_{0a}^{\text{RE}} + M_a^{\text{Cr}} = \frac{1}{2} g_a \mu_B N (\Delta/E_0) \tanh(E_0/2kT) + 3N \mu_B (\langle S_z \rangle / S) \sin \alpha, \quad (3)$$

In (3), we have taken $g = 2$ for the Cr^{3+} ions and $\langle S_z \rangle / S$ is the normalized average magnetic moment

per Cr^{3+} ion.

The constant canting angle assumption also implies that

$$\Delta = \Delta_0 \langle S_z \rangle / S, \quad (4)$$

where Δ_0 is the Cr^{3+} induced splitting at 0°K. The function $\langle S_z \rangle / S$ was taken from magnetization measurements on LuCrO_3 ,¹³ normalized to unity at $T = 0$ °K. Differences in T_N between LuCrO_3 and TbCrO_3 or PrCrO_3 were dealt with by using a reduced temperature scale T/T_N for each of the three compounds. Using the results of magnetization measurements on YCrO_3 ,¹⁴ or EuCrO_3 ,¹⁵ instead of those for LuCrO_3 gave the same results.

The Cr^{3+} contribution to the total susceptibility can also be obtained by taking corresponding results for YCrO_3 ,¹⁴ or LuCrO_3 ,¹³ after correcting for the different values of T_N .⁸ These yield an essentially temperature- and direction-independent contribution of about 5×10^{-3} emu/mole-Oe. In addition, there can be Van Vleck type contributions to the a and b direction principal susceptibilities from the elevated crystal-field states of the rare-earth ions. Their order of magnitude can be estimated from the measured c -axis susceptibilities, whose rare-earth contributions are entirely of the Van Vleck type. Since, as pointed out earlier, these are small, we shall neglect both the Cr^{3+} and Van Vleck contributions to χ_a^{RE} and χ_b^{RE} for the case of TbCrO_3 . However, for PrCrO_3 , where the measured susceptibilities are considerably smaller, we add to (2d) a temperature-independent susceptibility χ_0 to obtain final expressions for χ_a and χ_b . Similarly, for $M_a(H_a)$ and $M_b(H_b)$ we add to (2b) and (2c) the quantity $\chi_0 H_i$ ($i = a, b$).

Values for D , Δ_0 , $g_{\text{eff}} = (g_a^2 + g_b^2)^{1/2}$, $\phi = \arctan(g_a/g_b)$, α , and (for PrCrO_3) χ_0 were determined by fitting all the experimental data for each compound to the appropriate expressions. A computerized least-squares technique was employed to fit simultaneously all the experimental data for each material separately. The best fit was obtained with the values listed in Table I. In addition, for PrCrO_3 , we had $\chi_0 = (7.5 \pm 3) \times 10^{-3}$ emu/mole-Oe which is essentially equal to χ_c for this compound. The negative sign of α for the case of PrCrO_3 reflects the antiparallel alignment of the Cr and Pr contributions to the spontaneous magnetization. All errors quoted are statistical and indicate two standard deviations. A separate fit to only PrCrO_3 data in Figs. 1, 4, 5 did not result in any significant change in the best-fit parameters. Using the best-fit values, the total magnetization M_a and principal susceptibilities χ_a , χ_b were calculated as a function of temperature for both TbCrO_3 and PrCrO_3 . The results

TABLE I. D : crystal-field splitting; Δ_0 : Cr^{3+} -induced Zeeman splitting at the rare-earth ion site extrapolated to 0°K ; g_{eff} , ϕ : magnitude of the effective g factor and its angle with the b crystallographic axis.

	D (K°)	Δ_0 (K°)	g_{eff}	ϕ (deg)	α (mrad)
TbCrO_3	14 ± 1.5	1.8 ± 0.1	17.9 ± 0.4	43 ± 1.5	< 5
PrCrO_3	55 ± 5	17.8 ± 0.5	4.4 ± 0.3	47 ± 3	-18 ± 1
HoCrO_3^a	4 ± 2	14.7 ± 0.2	17.3 ± 0.3	25 ± 1	56 ± 12

^a Reference 8.

obtained are shown in Figs. 1–5. In addition, the calculated values of $M_a(H_a)$ and $M_b(H_b)$ for PrCrO_3 at 4.2°K are given in Fig. 6. Generally speaking, the fit is excellent, considering the various approximations employed in the analysis.

DISCUSSION

For TbCrO_3 we have found that the Cr^{3+} and Tb^{3+} spin structures are $F_x G_z$ and $f_x c_y$, respectively, from 4.2°K to $T_N = 167^\circ\text{K}$. This is in agreement with the results of neutron-diffraction measurements.^{2,3} The effective g factor of the Tb^{3+} lowest-lying pair of states lies in the $a-b$ crystallographic plane and is equal to 17.9. The maximum possible value of 18 would occur if the doublet was composed of pure $J_\zeta = \pm 6$ states of 7F_6 . (Here ζ refers to the local quantization axis parallel to the Tb^{3+} -induced moment.) We thus conclude that the doublet is basically the $J_\zeta = \pm 6$ states of the ground term. Our value of 17.9 is in agreement with studies of Tb^{3+} in TbFeO_3 , TbAlO_3 , and TbCoO_3 , from which g values of 17.7, 17.6, and 16.5, respectively, have been reported.¹⁶ For these compounds the angle between the g axis and b has been reported¹³ to be about 55° in comparison with the value of 43° obtained by us for TbCrO_3 . Finally, we have found that the canting angle α of the Cr^{3+} spin system in TbCrO_3 is unusually small. The same result has been reported from powder measurements.¹⁷

It is interesting to note that the 0°K doublet splittings of TbCrO_3 ($E_0 = 14.1^\circ\text{K}$) and HoCrO_3 [$E_0 = 15.2^\circ\text{K}$ (Ref. 8)] are essentially identical. However, as seen in Table I, the crystal-field-induced splitting is the dominant contribution to E_0 in the case of TbCrO_3 . For HoCrO_3 , on the other hand, the Cr-Ho coupling is the mechanism primarily responsible for the doublet splitting. This is reflected particularly in the differing temperature dependence of χ_a and χ_b for the two compounds. In the case of HoCrO_3 , both of these susceptibilities exhibit sharp maxima at 10°K while for TbCrO_3 they increase monotonically with decreasing temperature for all $T > 4.2\text{K}$. Note that the low-temperature ($4.2 < T < 15^\circ\text{K}$) zero-field magnetic

behavior of TbCrO_3 will be insensitive to a small rare-earth-rare-earth coupling term as the crystal-field splitting is the dominant contribution to E_0 .

Turning to PrCrO_3 , we have found that its spin structure is identical to that of TbCrO_3 from 4.2°K to T_N . No evidence for the $\text{Cr}^{3+} F_z G_x$ mode reported from 4.2°K neutron-diffraction studies² was found. The reason for this discrepancy may be a dependence of spin structure on sample shape, such as has been suggested for the case of TbFeO_3 .¹⁸ Such a dependence, however, is much less likely to occur in PrCrO_3 than in TbFeO_3 due to the factor-of-4 ratio in the 0°K saturation moment³ of Pr^{3+} ($2.2\mu_B$) as compared with Tb^{3+} ($8.8\mu_B$) for the respective compounds.

For PrCrO_3 , the effective g factor has been found to be 4.4. (The maximum value possible for a pair of crystal-field states of 3H_4 is 6.4.) This g factor lies in the $a-b$ crystallographic plane and the crystal-field splitting between the two lowest-lying states is, in our model, 55°K . This model thus differs sharply from that of Pataud and Sivardiere, who have reported that the effective g factor of the lowest-lying doublet is along the a axis¹⁹ and that the doublet splitting is approximately 0.2°K .⁷ Such a level scheme would indicate that our level at 55°K is an elevated singlet or doublet and that the two lowest-lying states are essentially degenerate. This is indeed the model suggested for the Schottky anomaly of 22°K in the specific heat of PrFeO_3 .⁷ While we cannot completely rule out this interpretation, it should be noted that studies of Pr^{3+} in²⁰ GdAlO_3 and²¹ YAlO_3 show no evidence of such degenerate crystal-field states.²⁰ Finally, an independent estimate of the splitting between the ground and excited levels (independent of whether they are both singlets or doublets) was obtained by fitting the limited ($1.5 < T < 5^\circ\text{K}$) specific-heat data for PrCrO_3 to the low-temperature tail of a Schottky-type anomaly.⁷ Assuming, in conformity with results obtained on other rare-earth orthochromites,²¹ that the Debye temperature of PrCrO_3 lies between 200 and 300°K , a splitting of $E_0 = 44 \pm 3^\circ\text{K}$ at 0°K was found. This is in fair agreement with

the corresponding value of 55 ± 5 °K found from our study.

To summarize, we have here reported on a study of the spontaneous magnetization and principal susceptibilities of TbCrO_3 and PrCrO_3 between 4.2 °K and their Néel temperatures. For PrCrO_3 the field dependence of the magnetization at $T = 4.2$ °K was also measured. For both materials we have found that (a) the Cr^{3+} spin system orders in an $F_x G_z$ mode, (b) no spin reorientation or compensation point occurs for 4.2 °K $\leq T \leq T_N$,

(c) the effective g tensor is essentially zero along the c crystallographic axis. All the magnetic data can be understood in terms of a doublet model for the lowest-lying pair of rare-earth ion crystal-field states.

ACKNOWLEDGMENT

We are indebted to Y. Chopin for invaluable technical assistance during the course of this work.

*Work supported in part by the Commission for Basic Research of the Israel Academy of Sciences and Humanities and was done in partial fulfillment of the Ph.D. requirements of one of the authors (J. D. G.).

¹S. Geller and E. A. Wood, *Acta Cryst.* **9**, 563 (1956); S. Geller, *J. Chem. Phys.* **24**, 1236 (1956); E. F. Bertaut and F. Forrat, *J. Phys. Rad.* **17**, 129 (1956).

²E. F. Bertaut, J. Mareschal, G. de Vries, R. Aleonard, R. Pauthenet, J. P. Rebouillat, and V. Zarubicka, *IEEE Trans. Mag.* **2**, 453 (1966); the value of $T_N = 118$ °K is in error, see E. F. Bertaut *et al.*, *J. Appl. Phys.* **37**, 1038 (1966), where $T_N = 158$ °K is cited for TbCrO_3 .

³E. F. Bertaut, J. Mareschal, and G. F. de Vries, *J. Phys. Chem. Solids* **28**, 2143 (1967).

⁴W. C. Koehler, E. O. Wollan, and M. K. Wilkinson, *Phys. Rev.* **111**, 58 (1960).

⁵E. F. Bertaut, in *Magnetism*, edited by G. T. Rado and H. Suhl (Academic, New York, 1963), Vol. III, p. 149.

⁶E. F. Bertaut, *Acta Crystallogr.* **A24**, 217 (1968).

⁷P. Pataud and J. Sivardiere, *J. Phys. (Paris)* **31**, 1017 (1970).

⁸R. M. Hornreich, B. M. Wanklyn, and I. Yaeger, *Int. J. Magn.* **2**, 77 (1972) (Part II); other papers in this series are S. Shtrikman, B. M. Wanklyn, I. Yaeger, *ibid.* **1**, 327 (1971) (Part I); R. M. Hornreich, B. M. Wanklyn, I. Yaeger, *ibid.* **4**, 313 (1973) (Part III), A. Hasson, R. M. Hornreich, Y. Komet, B. Wanklyn, and I. Yaeger, *Phys. Rev. B* **12**, 5051 (1975) (Part IV).

⁹P. J. Flanders and W. D. Doyle, *Rev. Sci. Instrum.* **33**, 691 (1962).

¹⁰Manufactured by "Ricor", Ein Harod-Ichud, Israel.

¹¹J. S. Griffith, *Phys. Rev.* **132**, 316 (1963).

¹²A. P. Malozemoff and R. L. White, *Solid State Commun.* **8**, 665 (1970).

¹³I. Yaeger, Ph.D. thesis (Weizmann Institute of Science, 1973) (unpublished); R. M. Hornreich, S. Shtrikman, B. M. Wanklyn, and I. Yaeger (unpublished).

¹⁴V. M. Judin and A. B. Sherman, *Solid State Commun.* **4**, 661 (1966).

¹⁵J. D. Gordon (unpublished).

¹⁶A. Kappatch, S. Quezel-Ambrunaz, and J. Sivardiere, *J. Phys. (Paris)* **31**, 369 (1970), and references cited therein.

¹⁷A. V. Apostolov and B. N. Tafrajdjeva, *C. R. Acad. Bulgare Sci.* **26**, 615 (1973).

¹⁸R. Bideaux, J. E. Bourée, and J. Hammann, *Phys. Lett. A* **40**, 167 (1972).

¹⁹P. Pataud and J. Sivardière, *J. Phys. (Paris)* **31**, 803 (1970).

²⁰J. Fengarol and N. Peltier-Allard, *C. R. Acad. Sci. (Paris)* **272**, 901 (1971).

²¹J. B. Ayasse, thesis (University of Grenoble, 1970) (unpublished); A. De Combarieu, J. Mareschal, J. C. Michel, J. Peyrard, and J. Sivardiere, *C. R. Acad. Sci. (Paris)* **267**, 1169 (1968).